Critical-Angle Transmission Gratings for High Resolution, Large Area Soft X-ray Spectroscopy

Response to NASA Solicitation NNH11ZDA018L,
Concepts for the Next NASA X-ray Astronomy Mission

Ralf K. Heilmann, Principal Research Scientist, MIT, ralf@space.mit.edu, 617-253-8764

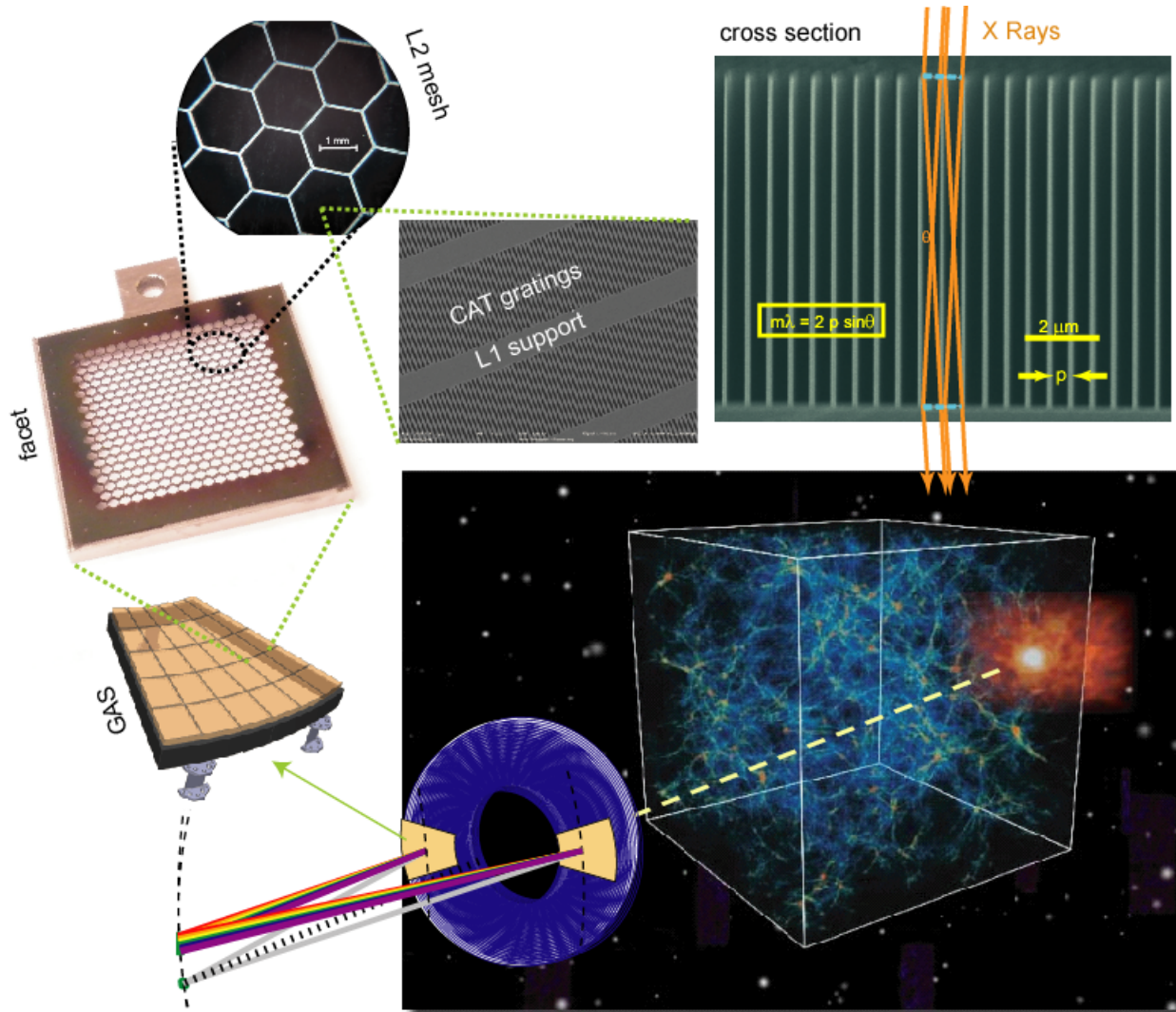|		
Mark W. Bautz, MIT	John E. Davis, MIT	Daniel Dewey, MIT
David P. Huenemoerder, MIT	Herman L. Marshall, MIT	Randall L. McEntaffer , Univ. of Iowa
Stephen L. O'Dell, NASA MSFC	Mark L. Schattenburg, MIT	Norbert S. Schulz, MIT
Randall Smith, SAO	William Zhang, NASA GSFC	

This White Paper is in response to NASA Solicitation NNH11ZDA018L from Sept. 13, 2011, Request for Information for "Concepts for the Next NASA X-ray Astronomy Mission". It falls into the "enabling technologies" category. RKH is willing to participate in and present at the workshop if invited.

1. Summary

The expression "spectroscopy puts the 'physics' into astrophysics" sums up the paramount importance of spectroscopy for the quantitative modeling of many astrophysical theories [1]. Not surprisingly, each of the "New Worlds New Horizons" (NWNH) Astro2010 Decadal Survey high priority science objectives that IXO could have fulfilled leads to demanding performance requirements for spectral resolution (small ΔE) and resolving power (large $R = \lambda/\Delta\lambda$). The x-ray band of interest for these science objectives extends over more than two orders of magnitude in energy. High quality spectroscopy over such a large band cannot be obtained with a single instrument. For example, imaging spectroscopy with a spectral resolution of 2 eV has been demonstrated with small transition-edge-sensor-based microcalorimeter arrays, providing resolution > 3000 for energies > 6 keV. Such microcalorimeter spectrometers are also well matched in angular resolution to long-focal-length telescopes with state-of-the-art point-spread functions on the order of 10" (HPD). However, towards longer wavelengths energy dispersive detectors cannot provide the spectral resolution that is required to address several of the NWNH high priority science objectives. In the crucial soft x-ray band that contains the lines of C, N, O, Ne and Fe ions *the only known technology capable of enabling high spectral resolving power is wavelength-dispersive, diffraction-grating-based spectroscopy.*

Recently developed Critical-Angle Transmission (CAT) grating technology – in combination with x-ray CCD cameras and large collecting-area focusing optics - will enable a new generation of soft x-ray spectrometers with unprecedented resolving power and effective area and with at least an order of magnitude improvement in figures-of-merit for emission and absorption line detection. It will be essential to answer a number of high-priority questions identified in NWNH and open the door to a new discovery space. CAT grating technology currently stands at TRL3 and is expected to mature to TRL5 within the next couple of years.

Another type of grating spectrometer that uses blazed reflection gratings in the extreme off-plane mount and addresses the same science priorities is described in a separate response to this RFI by McEntaffer.[2]

2. Science

Absorption and emission line spectroscopy with the performance made possible by a well-designed CAT x-ray grating spectrometer (CATXGS) will target science objectives concerning the large scale structure of the universe, cosmic feedback, interstellar and intergalactic media, and stellar accretion. Kinematics of galactic outflows, hot gas in galactic halos, black hole growth, the missing baryons in galaxies and the Warm Hot Intergalactic Medium, and the effect of x-ray radiation on protoplanetary disks all pose questions that will be addressed by a CATXGS-carrying mission. Several such mission concepts are described in separate responses to the above RFI, and the science questions and respective mission performance are discussed in more detail there.[3-5]

3. Grating Spectrometer Fundamentals

CAT gratings are essentially high-efficiency blazed transmission gratings.[6] An efficient spectrometer design originally developed for IXO is shown in Fig.1 for reference.[7] In the following we discuss the key optical design and technical parameters that lead to a high-spectral-resolving-power and high-effective-area grating spectrometer and in Section 4 how CAT gratings address these parameters.
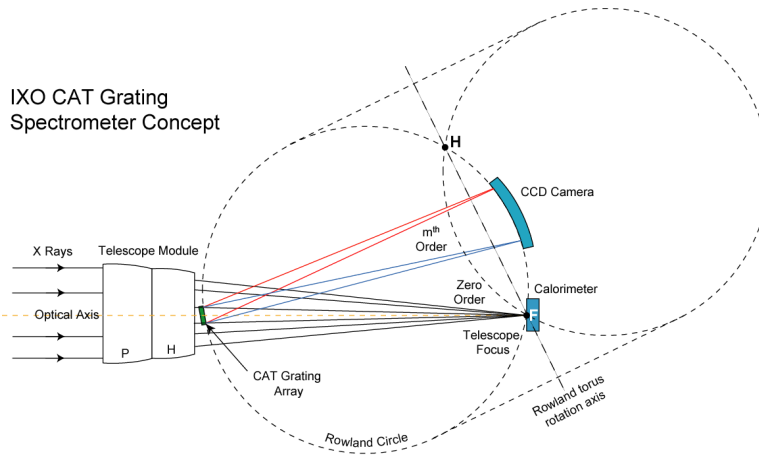
Fig.1: Optical design for a CAT grating spectrometer, utilizing sub-aperturing and a tilted Rowland torus.

3.1 Key ingredients for high spectral resolving power

A diffraction grating disperses incident photons into discrete diffraction orders according to wavelength. The simplest case is the well-known grating equation

$m\lambda/p = \sin\alpha - \sin\beta(\lambda)_m,$

where $m = 0, +/-1, +/-2,\ldots$ is the diffraction order, λ is the photon wavelength, p is the grating period, α is the angle of incidence onto the grating, and $\beta(\lambda)_m$ is the angle of diffraction for order m. The _resolving power increases with increasing diffraction angle_, which means with _longer wavelengths, higher diffraction orders, and smaller grating periods_. Of course this rule is subject to how much of the diffracted radiation ends up in a particular order, i.e. high orders are useless if they do not carry any photons.

In an objective grating spectrograph (Chandra High-Energy Transmission Grating Spectrometer (HETGS), XMM-Newton Reflection Grating Spectrometer (RGS)) diffraction peaks are broadened by the telescope point-spread function (PSF). Therefore the _resolving power increases with improving telescope angular resolution_ until spectrometer aberrations and other imperfections limit further improvements. In addition, since the plate scale of the telescope PSF is fixed in size, it is advantageous to increase the size of the dispersed spectrum by _maximizing the dispersion distance between gratings and spectrometer readout._

X-ray telescopes generally utilize grazing incidence mirrors to focus incident light. Imperfections in the mirrors (figure errors, surface roughness) lead to angular deviations and scattering from the ideal direction of specular reflection. At grazing incidence this leads to anisotropic broadening of the reflected beam (strong broadening in the plane of incidence, reduced broadening in the plane perpendicular to the plane of incidence).[8] The PSF of a typical Wolter-I telescope consists of the azimuthal (around the optical axis) integral over all planes of incidence and is therefore dominated by the strong broadening. However, if gratings intercept only a small azimuthal range of mirrors (a sub-aperture of the total aperture) one can orient the grating dispersion direction in the direction normal to the plane of incidence, which is subject to reduced broadening. The sub-apertured Line-Spread-Function (LSF) of a spectral line, which is the projection of the 2-D PSF onto the grating dispersion axis, can therefore be much reduced

compared to the width of the full telescope PSF. Thus *azimuthal sub-aperturing can be used to increase spectral resolving power*.

On the detector side *the spatial resolution of the readout detector has to be fine enough to oversample the width of a spectral line*. In addition, if the required spectral bandwidth exceeds the free spectral range of the gratings, neighboring diffraction orders with different wavelengths will spatially overlap, and *the detector must be able to distinguish between these orders ("order-sort")*.[9] Both of these requirements are met by existing x-ray CCDs.

3.2 Key ingredients for high effective area

Due to the faintness of most celestial x-ray sources, considerable technological effort has to be made in order to maximize collecting area. The starting point is the geometrical aperture of the telescope, which is obviously limited by available mass and cost. Once the aperture is set, every surface that a soft x-ray interacts with should be optimized for maximum yield and minimum absorption. Mirror design needs to take into account desired bandwidth and effective mirror area as a function of wavelength. This often entails complex trades between graze angles, focal length, mirror mass, number of segments (in the case of segmented optics) and cost. For a grating spectrometer high effective area means that *grating diffraction efficiency should be maximized over the spectral range of interest* and that any necessary *mechanical support structures that absorb x rays should be minimized*. The detector needs to be of highest possible quantum efficiency, and optical blocking filters should be as thin as possible.

3.3 Soft X-ray Diffraction Gratings:

Soft x-ray diffraction gratings fall into two main categories: Transmission gratings and reflection gratings. Transmission grating spectrometers have the advantage of being insensitive to grating misalignments and non-flatness. X-ray transmission gratings are also very thin and therefore light-weight, and they become highly transparent at higher energies, which allows harder x rays to be collected at the imaging focus by,
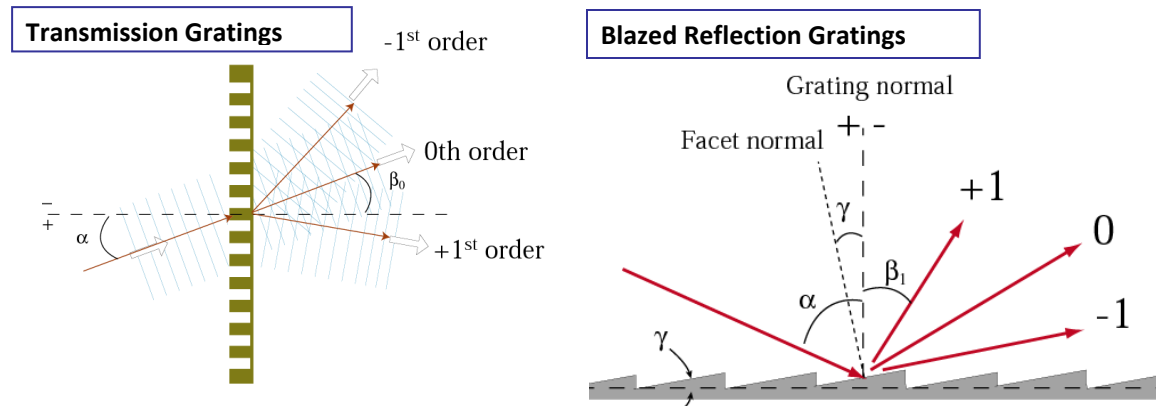

Fig. 2: Comparison of transmission gratings and blazed reflection gratings.

for example, a microcalorimeter imaging spectrometer as in the case of IXO and AXSIO. The main drawbacks of previous generations of x-ray transmission gratings were their relatively low diffraction efficiency in the soft x-ray band (caused mainly by absorption in the grating materials) and low dispersion limited by the difficulty of fabricating gratings with small periods. Reflection gratings have the advantage that they can be blazed for higher orders, which increases dispersion, and that diffraction efficiency can be high due to the use of small angles of grazing incidence. Also, for the in-plane

reflection gratings in the RGS on XMM-Newton the grating period is effectively reduced through the use of its small graze angle geometry.[10] The drawbacks of grazing-incidence reflection gratings are that they are very sensitive to alignment and figure errors, and that they need to be long in the direction of propagation in order to intercept a given mirror aperture. Both drawbacks lead to relatively long and thick grating substrates and significantly more mass per mirror area than transmission gratings.

X-ray gratings have a long heritage in high-energy astrophysics, going back to the Bragg Crystal Spectrometer on Ariel V and Einstein Observatory's Objective Grating Spectrometer. The HETGS on Chandra uses phase-shifting gold bar transmission gratings supported by polyimide membranes.[11] The transmission geometry prevents the gratings from degrading the unsurpassed 0.5" angular resolution of the Chandra optics and leads to resolving powers up to R ~ 1000, albeit with small effective area (< 50 cm^2 for E < 1 keV), in part due to the absorbing membranes. The RGS uses blazed reflection gratings in the in-plane mount geometry. The larger dispersion compensates for the larger telescope PSF, and the lack of absorption gives rise to effective area > 50 cm^2 up to much longer wavelengths than the HETGS.

4. Critical-Angle Transmission (CAT) Gratings

CAT gratings represent a recent breakthrough development at MIT's Space Nanotechnology Lab, enabled mostly by NASA ROSES APRA support.[12,13] They are *blazed transmission gratings that combine the advantages of both transmission and reflection gratings*. The implementation of CAT gratings in state-of-the-art x-ray telescopes will lead to significant gains in effective area and resolving power with minimum use of resources (mass, power, cost). Blazing is achieved in analogy to blazed reflection gratings through incidence onto a smooth grating surface at a small angle of grazing incidence. The main difference lies in the fact that the reflecting surfaces in the CAT grating are the sidewalls of the thin, high-aspect-ratio grating bars that are freely suspended at their narrow sides by support structures from within the plane of the grating (see Fig. 3). The geometrical parameters of the grating bars are given by the small angles of grazing incidence, the desire to have each photon incident on the gap between two bars undergo a single "reflection" (in a geometrical optics approximation), and minimum grating duty cycle (ratio of bar thickness to grating period) for maximum throughput. For IXO a straw man set of geometrical grating parameters was p = 200 nm, b = 40 nm, α = 1.5 deg, and d = a/tanα = 6.11 μm. This means that the grating bar aspect ratio b/d is on the order of 150.
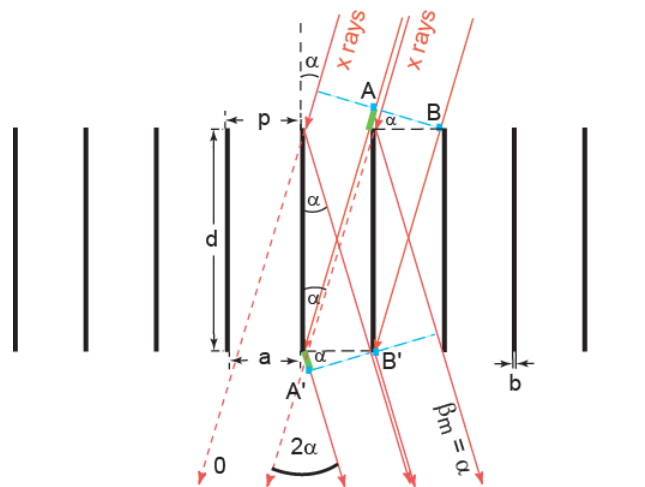

Fig. 3: Schematic of the basic CAT grating concept. (Support structures not shown.)

Modeling of such structures predicts large efficiency gains over HETGS gratings (Fig. 4) Most of the diffraction efficiency ends up in a small number of (either positive or negative) diffraction orders under a "blaze envelope", which is centered at an angle 2α from the path of photons transmitted in 0th order.[9,14] If gratings are placed in the converging beam of a telescope similar to the case of the HETGS on Chandra, the spectral resolving power (before sub-aperturing) can simply be estimated by dividing the distance of a given diffraction order from focus by the width of the telescope PSF. This distance is proportional to 2α at the peak of the blaze and has the effect that the efficiency-weighted resolution is fairly constant across the band pass (shorter wavelengths contribute in higher orders, longer wavelengths contribute in lower orders) [6,14]. The band pass is limited towards shorter wavelengths when the chosen value of α exceeds the critical angle for total external reflection $\alpha_c(\lambda)$.
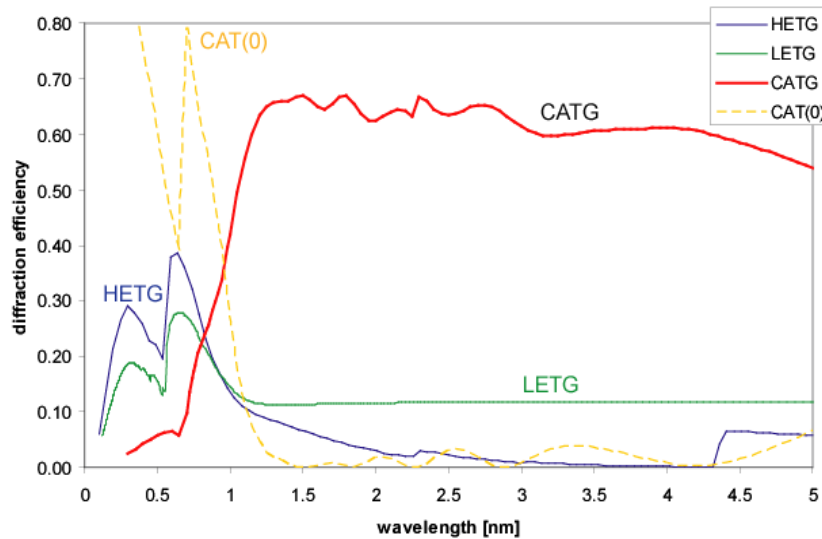

Fig. 4: Diffraction efficiencies for *Chandra* HETG and LETG (Low Energy Transmission Gratings), and for a 200 nm-period silicon CAT grating. "CAT(0)" shows the CAT grating 0th order transmission, which contributes to the effective area at the imaging focus.

4.1 CAT Grating Spectrometer Design Considerations

Material choice: The only material that is currently known to be amenable to fabrication of such small structures with such extreme geometries and smoothness is silicon.[15,16] This choice sets the index of refraction and thus the behavior of $\alpha_c(\lambda)$. For example, for $\alpha = 1.5$ deg the reflectivity would fall below 50% for $\lambda < 1.1$ nm.

Grating period: Since CAT gratings are blazed, the relevant dispersion is given by the orders that fall into the blaze envelope. For a fixed blaze angle the dispersion is therefore fairly independent of the grating period (shorter period gratings will blaze in lower orders). However, shorter periods will lead to broader blaze envelopes ("single slit diffraction"), which can have an effect on the length of the readout camera. Furthermore, if the period is too large, then the grating will blaze in very high orders and the energy resolution of the readout detector might not be sufficient to separate spatially overlapping orders. A period of 200 nm seems to be close to optimal.

Blaze angle: The blaze angle sets the dispersion and the short-wavelength cutoff. Large blaze angles lead to large dispersion and resolving power, but also shift the cutoff to longer wavelengths. For example, for

α = 1.5 deg a 200 nm period grating (same as Chandra HETG) would blaze in 10th order at ~ 1.2 keV, providing ten times the dispersion of the HETG in first order. The blaze angle together with the grating bar width sets the aspect ratio for the grating bars. Higher aspect ratios are more challenging to fabricate.

Grating depth: This is given by the choices for period and blaze angle.

Grating bar width: The grating bars should be as thin as possible to maximize transmission or diffraction efficiency. If they are too thin the grating bars will become too weak and collapse.

Sub-aperturing: Limiting grating coverage to a fraction of a full (cylindrically symmetric) Wolter-I optic and dispersing normal to the average plane of incidence for this sub-aperture will narrow the spectral LSF and increase resolving power. Detailed ray-trace studies have shown that sub-aperturing to 30 deg in azimuth can improve resolving power by factors of 3-4, [7] even for a 10" telescope PSF. Two diametrically opposed sub-apertures can produce a single spectrum or at least share a single readout. Covering a whole optic with 2 x 30 deg sub-aperture pairs would require six separate readouts.[3]

4.2 Maximizing Scientific Yield with the Use of CAT Gratings

CAT gratings enable an order of magnitude improvement in soft x-ray spectroscopy figures of merit compared to currently operating instruments (see Fig. 5 as an example).
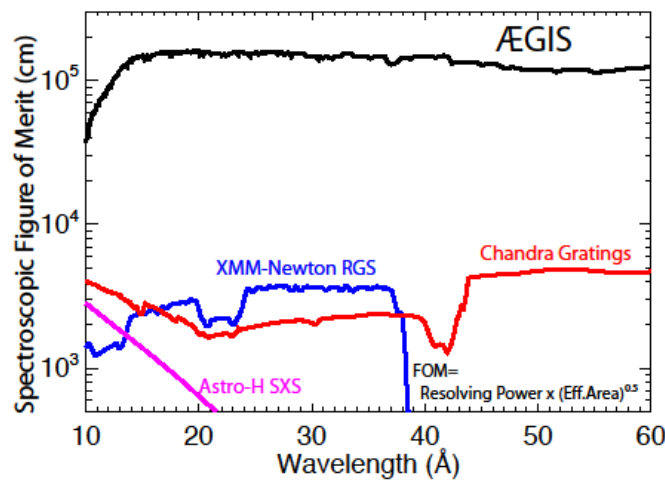

Fig. 5: Figure of merit for the accuracy of line centroid (velocity) measurements for existing instruments and the AEGIS mission.[3]

Using IXO parameters as example, blazing at 2α = 3 deg provides up to *ten times the dispersion* of the Chandra HETGS. With the low mass of CAT grating facets (0.1-0.3 g/cm^2) one can afford to cover large telescope apertures at maximum distance from focus, which *maximizes the dispersion distance between gratings and spectrometer readout.* The combination of large blaze angle, long dispersion distance, and moderate sub-aperturing can provide R > 3000 over a broad band (E < 1 keV) even for a telescope with 10" PSF.[3,4] This is to be compared with the XMM RGS, which only achieves R < 200 at 0.9 keV with a ~ 12" PSF telescope.

CAT gratings provide high diffraction efficiency over a broad wavelength band – more than five times higher than even the Chandra LETG over the 1-5 nm wavelength range. This assumes that soft x-ray absorbing support structures (L1 supports, L2 supports, facet frames) do not block more than 10% of the area per level. A well-designed spectrometer can thus be expected to yield up to 40-45% of the mirror collecting area that is fed into a CAT grating array (before detector losses).[17] (An added advantage of

placing CAT gratings near the telescope mirrors is that they can benefit from the mirror temperature control and do not require a separate temperature control system.[7])

4.3 CAT Grating X-Ray Spectrometer (CAT-XGS) Concepts

A number of CAT-XGS concepts have been studied over the last few years, some in considerable detail. The CAT-XGS for IXO underwent a multi-year design and cost study, resulting in an extensive Payload Definition Document [14] and a number of publications.[6,7,9,15] Three of the concepts listed below have the same basic setup: Two diametrically opposed sub-apertures of a Wolter-I mirror of 30 deg in azimuth each are covered by an array of 60x60 mm^2 CAT gratings. Both arrays diffract onto the same linear readout CCD array. Gratings, CCDs, and telescope focus are placed on the same Rowland torus. The AEGIS mission concept employs a total of six sub-aperture pairs with a 10" telescope PSF and has a novel feature that might be particularly interesting.   Since the narrowing of the PSF also applies to the 0th order image, one may arrange the sub-apertured images for each sector pair to be detected independently to take advantage of the 2-3 arcsec imaging of the mirrors in one dimension.   By sampling six position angles, an image may be reconstructed with 2-3 arcsec resolution from a 10" optic. This might be especially useful for extended sources.[3]

Mission	Optic PSF [arcsec]	Focal length [m]	CAT-XGS eff. area [cm^2]	Sub-aperture (azimuth) [deg]	Resolving power E/ΔE
IXO	5	20	> 1000	2 x 30	~ 3500-4000
AXSIO	10	10	> 1000	2 x (2 x 30)	> 3000
AEGIS	10	4.4	~ 1400	6 x (2 x 30)	~ 3000-4000
SMART-X	0.5	10	~ 4000	1 x 360	> 4000

Table 1: Mission concepts with a CAT-XGS and expected performance.

5. Grating Fabrication and Demonstrated Performance

In the following we review the status of CAT grating fabrication and testing.

5.1 Wet Etch

We started to investigate CAT grating fabrication less than six years ago.[16,17] Fabrication starts with a <110> silicon-on-insulator (SOI) wafer with a device layer thickness equal to the desired grating depth. The device layer (front side) is patterned with the 200 nm-period CAT grating pattern aligned to the <111> Si crystal planes, using our Nanoruler tool.[18] An orthogonal support mesh (L1 supports - period ~ 5 – 30 μm) is also patterned into the front side mask. Large (mm-sized) holes are etched into the back side until the buried oxide (BOX) layer is reached. Anisotropic wet etching in KOH solution is used to simultaneously etch CAT gratings and L1 supports into the device layer, again using the BOX layer as an etch stop. The high etch anisotropy leaves narrow and tall CAT grating bars with almost atomically smooth <111> sidewalls. However, the L1 support mask prevents inclined <111> planes from being etched. This leads to broadening of the L1 supports with increasing etch depth and a strongly trapezoidal L1 support bar cross section. The L1 mesh period cannot be arbitrarily large due to mechanical considerations, and therefore valuable CAT grating area is lost to L1 supports. Finally, the BOX layer is removed via an HF etch, and the sample is dried in a supercritical dryer to avoid surface-tension-induced

collapse. Using this approach we have successfully demonstrated the fabrication of CAT gratings with the geometrical parameters of the above IXO straw man design.

5.2 X-ray performance

Several CAT grating samples were tested at a synchrotron beam line.[9,12,15,19] The gratings performed in accordance with theoretical predictions over a large range of wavelengths (0.96 – 49 nm), achieving 80-100% of theoretical efficiency over most of the band after correcting for the presence of the trapezoidal L1 mesh bars. This result puts CAT grating technology at TRL3.

5.3 Dry (Plasma) Etch

In order to minimize the area lost to L1 supports we started research on etch processes with the potential for high etch anisotropy that is independent of Si crystal lattice orientation. We settled on a Deep Reactive-Ion Etch (DRIE) process that rapidly alternates between SF_6 etch and C_4F_8 passivation steps.[20] The alternating steps allow the etching of high-anisotropy trenches, but the sidewalls suffer from well-known "scalloping". We have recently been able to approach our challenging grating bar geometry with DRIE, but this has required one of the most advanced tools available at present, an STS Pegasus etcher at the University of Michigan. We have shown that we can simultaneously transfer the CAT grating and L1 mesh patterns into the SOI device layer and stop at the BOX layer without significant broadening of the L1 supports. This crucial step now allows us to fabricate CAT gratings with maximum open area and minimal losses from the integrated L1 support mesh. While small by DRIE standards, the remaining roughness on the CAT grating bar sidewalls will seriously reduce diffraction efficiency. We are currently developing a process that will reduce that roughness using a short "polishing" (wet etch) step in KOH, followed by critical-point drying.

5.4 Large-Area Gratings

Gratings should be as large as the spectrometer design allows in order to minimize the complexity and number of gratings needed for a grating array. The etched μm-thick device layer is too thin to support a membrane for a grating that is many cm in size. We have designed and fabricated hexagonal L2 support meshes that are etched out of the roughly 0.5 mm thick SOI handle layer (back side). Performing successful deep etches on both sides of the SOI wafer is a complex process that we only recently
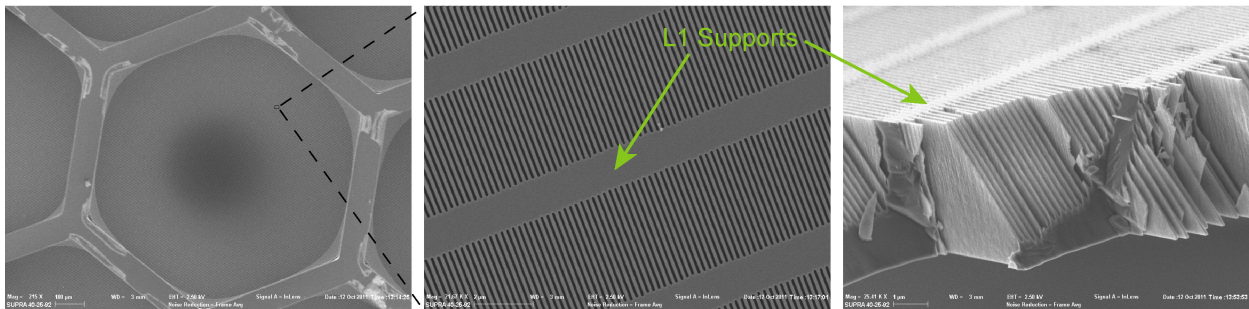

Fig. 6: Scanning electron micrographs (SEMs) of a recently fabricated (25 mm)^2 CAT grating with the full structural complexity of a CAT grating membrane. (Left) Bottom view of the hexagonal L2 support mesh. The mesh period is 1 mm, and the hexagon walls are 100 μm thick (81% open area) and 500 μm tall. (Middle) Same image, but zoomed in onto the 4 μm thin device layer with free-standing, 200 nm-period CAT grating bars that are suspended from the integrated L1 supports. 75% of the area is taken up by CAT gratings. (Right) Cleaved cross section from the same sample, showing CAT gratings and L1 supports etched all the way through the SOI device layer.

mastered.[21] Fig. 6 has new results that show for the first time a large ($> 25 \times 25$ cm^2) CAT grating with the full structural complexity of free-standing CAT grating bars with an integrated L1 mesh etched from the device layer and a L2 mesh etched from the back. A final KOH polish will turn this into a functioning large-area, high-throughput CAT grating membrane.

5.5 Grating Facets and Grating Array Structure

An array of gratings will be needed to achieve large effective area. Such an array typically consists of a Grating Array Structure (GAS) that holds individual grating facets in their proper position and orientation according to the spectrometer optical design. A grating facet consists of a grating membrane that is glued to a thin metal frame, which serves as the mechanical interface between the Si membrane and the GAS.[9] The mechanical strength and relevant resonances of a grating facet will be dominated by the L2 support mesh and the facet frame. We have begun to model and test the mechanical properties of 37x37 mm^2 Si membranes (consisting of just L2 supports) and prototype frames for compatibility with launch loads (see Fig. 7).[21]
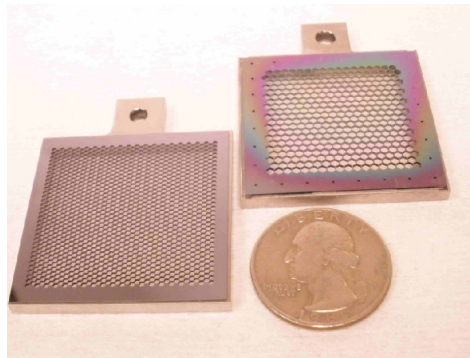

Fig. 7: Two prototype facets for vibration tests, consisting of an L2-only silicon membrane and a metal frame.

6. Future Work

6.1 Near term goals

Bring CAT grating technology to TRL5 by the end of 2013. We consider the following steps (not necessarily to be performed sequentially) as necessary and sufficient to reach that goal:

KOH polish: We need to demonstrate that we can reduce the roughness of dry-etched grating bar sidewalls sufficiently in order for the CAT gratings to have high diffraction efficiency.

Minimize supports: We have fabricated L1 supports with widths as small as 8% of the L1 mesh period. The required additional processing steps need to be added to the overall fabrication process. We have also fabricated stand-alone L2 meshes with up to 90% open area. For maximum effective area both L1 and L2 supports must be minimized in a single sample.

Mechanical design: We will continue initial finite element modeling to optimize facet frame and L2 mesh design for maximum stiffness with minimal mass and x-ray blockage.

Vibration, shock, thermal tests: We will analyze initial tests and reconcile the results with modeling. Tests and modeling will be iterated.

Resolution tests: We will test resolving power of prototype gratings in a suitable breadboard x-ray setup. We consider a successful test to demonstrate TRL4.

We consider successful environmental testing of CAT grating breadboard to bring us to TRL5. The definition of TRL6 will be mission specific. An example would be to increase grating size from the current 25x25 mm^2 up to 60x60 mm^2. We also plan to develop an improved frame-to-membrane alignment and bonding method based on Chandra technology.

6.2 Extensions beyond current designs

CAT grating fabrication so far has relied on the capability to etch silicon crystals in highly anisotropic fashion to achieve ultra-high aspect ratio grating bars with sub-nm smooth sidewalls. Relying on silicon for grazing incidence reflection directly couples the critical angle for a given wavelength to the reflectivity of silicon, and determines the maximum allowed angle of incidence for a desired band pass. It would be highly advantageous if the grating bar sidewalls could be made out of a higher-Z material, such as tungsten or ruthenium for example. This could be achieved through the decades-old technique of Atomic Layer Deposition (ALD) [22]. For Ru, α could be increased to 2.5 – 3.0 deg for 1 keV photons [23], resulting in increased blaze angles/dispersion/resolving power and lower grating bar aspect ratios, which are easier to fabricate. Alternatively one could stay at 1.5 deg. and expand the band pass to higher energies (E ~ 2.4 keV), where gratings can still supply higher resolution than a microcalorimeter with ΔE = 2eV.

6.3 Thoughts on risk and cost – the importance of continuous technology development

Starting from an idea and an initially unfunded fabrication effort we have made rapid progress in CAT grating development within a short time, approaching TRL4. Development so far has been predominantly supported through the ROSES APRA program, supplemented by internal MIT/Kavli Instrumentation and Development funds. Combined with a recently awarded NASA SAT grant to start next year we have been (and will continue to be) able to systematically attack technological challenges and gradually build a fabrication, software, and metrology infrastructure at modest cost that can serve as the foundation and model for eventual flight hardware fabrication. Such relatively small, but steady investment over more than just a few years in a very promising technology brings two important advantages: It matures technology long before mission start, thereby greatly reducing both risk and estimated mission development cost. In a very real sense, NASA technology development spending is not only an investment in, but also a down payment on, future mission development. While we welcome the competition for research funding and believe it serves the interests of NASA and the research community, ideally the above extremely competitive funding process should be replaced – at least partially – by a more predictable, continuous, and focused technology development funding process, since missing out on a single round of opportunities will stall progress, and two misses in a row can mean the end of a whole program.

APPENDIX - **References:**

[1] See for example C.R. Canizares,
http://cxc.harvard.edu/xgratings07/agenda/presentations/Canizares_Claude.pdf

[2] R. L. McEntaffer *et al.*, "Reflection Grating Spectrometers," Enabling Technology Response to the Concepts for the Next NASA X-ray Astronomy Missions RFI, Solicitation: NNH11ZDA018L.

[3] M. W. Bautz *et al.*, "AEGIS, an Astrophysics Experiment for Grating and Imaging Spectroscopy," Mission Concept Response to the above RFI.

[4] J. Bookbinder *et al.*, "The Advanced X-Ray Spectroscopic Imaging Observatory," Mission Concept Response to the above RFI.

[5] A. Vikhlinin *et al.*, "SMART-X, Square Meter Arcsecond Resolution X-Ray Telescope," Mission Concept Response to the above RFI

[6] K. Flanagan *et al.*, Spectrometer Concept and Design for X-Ray Astronomy Using a Blazed Transmission Grating, *Proc. SPIE* **6688**, 66880Y (2007).

[7] R. K. Heilmann *et al.*, Critical-Angle Transmission Grating Spectrometer for High-Resolution Soft X-Ray Spectroscopy on the International X-Ray Observatory, Proc. SPIE **7732**, 77321J (2010).

[8] W. C. Cash Jr., "X-ray optics 2: A technique for high-resolution spectroscopy," *Appl. Opt.* **30**, 1749-1759 (1991).

[9] R. K. Heilmann *et al.*, Development of a Critical-Angle Transmission Grating Spectrometer for the International X-Ray Observatory, Proc. SPIE **7437**, 74370G (2009).

[10] J. W. den Herder *et al.*, "The reflection grating spectrometer on board XMM-Newton," *Astr. & Astroph.* **365**, L7-L17 (2001).

[11] C. R. Canizares *et al.*, "The Chandra high-energy transmission grating: Design, fabrication, ground calibration, and 5 years in flight," *PASP* **117**, 1144-1171 (2005).

[12] R. K. Heilmann, M. Ahn, E. M. Gullikson, and M. L. Schattenburg, Blazed High-Efficiency X-Ray Diffraction via Transmission through Arrays of Nanometer-Scale Mirrors, Opt. Express **16**, 8658 (2008).

[13] R. K. Heilmann, M. Ahn, and M. L. Schattenburg, Nanomirror Array for High-Efficiency Soft X-Ray Spectroscopy, SPIE Newsroom, doi: 10.1117/2.1200808.1235 (Aug. 14, 2008).

[14] http://sci.esa.int/science-e/www/object/index.cfm?fobjectid=44697

[15] R. K. Heilmann, M. Ahn, and M. L. Schattenburg, Fabrication and Performance of Blazed Transmission Gratings for X-Ray Astronomy, Proc. SPIE **7011**, 701106 (2008).

[16] M. Ahn, R. K. Heilmann, and M. L. Schattenburg, Fabrication of Ultrahigh Aspect Ratio Freestanding Gratings on Silicon-on-Insulator Wafers, J. Vac. Sci. Technol. B **25**, 2593 (2007).

[17] M. Ahn, R. K. Heilmann, and M. L. Schattenburg, Fabrication of 200 nm-Period Blazed Transmission Gratings on Silicon-on-Insulator Wafers, J. Vac. Sci. Technol. B **26**, 2179-2182 (2008).

[18] R. K. Heilmann, C. G. Chen, P. T. Konkola, and M. L. Schattenburg, Dimensional Metrology for Nanometer-Scale Science and Engineering: Towards Sub-Nanometer Accurate Encoders, Nanotechnology **15**, S504 (2004).

[19] R. K. Heilmann *et al.*, Diffraction Efficiency of 200 nm Period Critical-Angle Transmission Gratings in the Soft X-Ray and Extreme Ultraviolet Wavelength Bands, Appl. Opt. **50**, 1364-1373 (2011).

[20] P. Mukherjee *et al.*, Plasma Etch Fabrication of 60:1 Aspect Ratio Silicon Nanogratings with 200 nm Pitch, J. Vac. Sci. Technol. B **28**, C6P70-5 (2010).

[21] R. K. Heilmann *et al.*, Fabrication Update on Critical-Angle Transmission Gratings for Soft X-Ray Grating Spectrometers, Proc. SPIE **8147**, 81471L (2011).

[22] See for example http://www.cambridgenanotech.com/klc/scientificabstracts.php

[23] http://henke.lbl.gov/optical_constants/mirror2.html